Pharmacogn. Mag.
A multifaceted peer reviewed journal in the field of Pharmacognosy and Natural Products
www.phcog.com | www.phcog.net

ORIGINAL ARTICLE

Genotoxic Assay of Silver and Zinc Oxide Nanoparticles Synthesized by Leaf Extract of *Garcinia livingstonei* T. Anderson: A Comparative Study

Azharuddin B. Daphedar, Siddappa B. Kakkalameli[1], Govindappa Melappa[1], Tarikere Chandrashekharappa Taranath[2], Chandrashekar Srinivasa[3], Chandan Shivamallu[4], Asad Syed[5], Najat Marraiki[5], Abdallah M. Elgorban[5], Ravindra Veerapur[6], Sharangouda S Patil[7], Shiva Prasad Kollur[8]

Anjuman Arts, Science and Commerce College, Vijayapura, [1]Department of Botany, Davangere University, Shivagangotri, Davangere, [2]Environmental Biology Laboratory, P. G. Department of Studies in Botany, Karnatak University, Dharwad, [3]Department of Studies in Biotechnology, Davangere University, Shivagangotri, Davangere, [4]Department of Biotechnology and Bioinformatics, School of Life Sciences, JSS Academy of Higher Education and Research, Mysore, Karnataka, India, [5]Department of Botany and Microbiology, College of Science, King Saud University, P.O. 2455, Riyadh 11451, Saudi Arabia, [6]Department of Metallurgy and Materials Engineering, Malawi Institute of Technology, Malawi University of Science and Technology, Limbe, Malawi, [7]ICAR-National Institute of Veterinary Epidemiology and Disease Informatics (NIVEDI), Yelahanka, Bengaluru, [8]Department of Sciences, Amrita School of Arts and Sciences, Amrita Vishwa Vidyapeetham, Mysuru Campus, Mysuru, Karnataka, India

Submitted: 30-Dec-2020 Revised: 23-Feb-2021 Accepted: 27-Mar-2021 Published: 10-Jun-2021

ABSTRACT

Background: Green synthesis of metal and metal oxide nanoparticles (NPs) using plant extract performs a significant role as it is a promising alternative to the conventional chemical method in nanotechnology. **Aims:** In this paper, we report an environmentally benign method for the synthesis of silver nanoparticles (AgNPs) and zinc oxide nanoparticles (ZnONPs) using leaf extract of Garcinia livingstonei, and their mitotic activities were investigated using the root tip of Cicer arietinum. **Objectives:** The as-prepared NPs were characterized by ultraviolet-visible spectroscopy, infrared spectroscopy (FT-IR), X-ray diffraction (XRD), atomic force microscopy (AFM), and high-resolution transmission electron microscopy (HR-TEM). Analysis of FT-IR spectrum revealed that certain functional groups behaved as reducing and stabilizing agents in the formation of nanostructures. The crystalline nature of the AgNPs and ZnONPs was confirmed by XRD analysis. The size and shape of the as-obtained materials were found using HR-TEM analysis and were in the range of 5–65 nm and 38–94 nm for AgNPs and ZnONPs, respectively. Further, the root cells of C. arietinum were treated with both AgNPs and ZnONPs in different concentrations (5, 25, 50, and 100 µg/ml) for 24 h at the interval of 3, 6, 12, and 24 h along with distilled water as control. **Results:** The study clearly indicated that the AgNPs and ZnONPs showed an inhibitory effect on the cell division in root tip cells and caused a decrease in their mitotic index (MI) values. The reduction in MI in AgNPs is more evident than that of ZnONPs when compared to control. Aberrations in chromosomal behavior such as micronucleus, sticky chromosomes, bridges, multipolar anaphase, laggard, and c-metaphase were also observed. **Conclusion:** From the results, it is evident that the percentage of MI is inversely proportional, and chromosomal aberrations (CAs) are directly proportional to the concentration and duration of exposure.

Key words: Silver nanoparticles, chromosomal aberrations, Garcinia livingstonei, mitotic index, zinc oxide nanoparticles

SUMMARY

- We have prepared silver nanoparticles (AgNPs) and zinc oxide nanoparticles (ZnONPs) via eco-friendly method using *Garcinia livingstonei* leaf extract. The morphology of the synthesized AgNPs is found in the range of 5 to 65 nm and ZnONPs were between 38 and 94 nm with a spherical nature. The higher concentration of AgNPs had a marked decline in mitotic index and was found to be associated with a significant increase in abnormality index when compared to ZnONPs. Both the prepared NPs caused major changes in intracellular components into the root cell, leading to remarkable damage to the DNA and cell division. Moreover, both the NPs arrest the cell division at various phases of cell cycle and induce the formation of chromosomal abnormalities such as micronucleus, sticky chromosomes, bridges, multipolar anaphase, laggard, and c-metaphase. Therefore, it can be concluded that the synthesized ZnONPs were found to be more effective genetically as well as environmentally safe and nontoxic than the AgNPs.

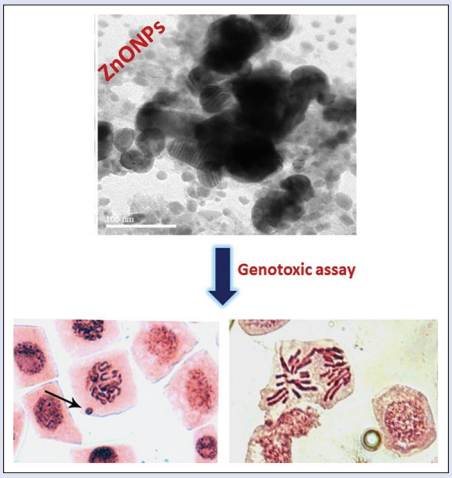

Abbreviations used: AgNPs: Silver nanoparticles; ZnONPs: Zinc oxide nanoparticles; FT-IR: Infrared spectroscopy; XRD: X-ray Diffraction; AFM: Atomic force microscopy; HR-TEM: High-resolution transmission electron microscopy; MNi: Micronuclei.

Correspondence:

Dr. Shiva Prasad Kollur,
Department of Sciences, Amrita School of Arts and Sciences, Mysore- 570 026, Karnataka, India.
Amrita Vishwa Vidyapeetham, Mysore - 570 026, Karnataka, India.
E-mail: shivachemist@gmail.com
DOI: 10.4103/pm.pm_536_20

Access this article online
Website: www.phcog.com
Quick Response Code:

Cite this article as: Daphedar AB, Kakkalameli SB, Melappa G, Taranath TC, Srinivasa C, Shivamallu C, *et al.* Genotoxic assay of silver and zinc oxide nanoparticles synthesized by leaf extract of *Garcinia livingstonei* T. Anderson: A comparative study. Phcog Mag 2021;17:S114-21.

INTRODUCTION

Nanotechnology has emerged extensively in various fields of applied sciences, dealing with the design, synthesis, and manipulation of new materials with approximate sizes from 1 to 100 nm.[1]At present, fabrication of nanoparticles (NPs) could be used for various potential applications, such as energy, environment, food processing, DNA sequencing, cosmetics, pharmaceuticals, agriculture, and innovative textile production, as well as several biomedical applications.[2,3] The synthesized silver and zinc oxide nanoparticles (ZnONPs) have gained significant attention due to their good chemical stability, catalytic activity, optoelectronics and photonics, unique ultraviolet (UV) filtering, and antifungal and antibacterial properties in the field of biomedical sciences.[4,5]

During the last few decades, a number of processes are available for the synthesis of metal NPs such as physical, chemical, and biological methods. Physical and chemical methods are often expensive, toxic, and produce hazardous chemicals during their synthesis.[6] However, biological methods are more reliable, nontoxic, and offer numerous benefits due to their low toxicity in comparison with the NPs prepared by chemical methods.[7] The use of biomaterials like plants (such as leaves, flower, stem bark, fruit peels, and seed) can be used to reduce metal ions to metal NPs in a single-step green synthesis process.[8] The phytochemicals (e.g., flavonoids, alkaloids, terpenoids, amides, and aldehydes) present in the leaf extract may act as reducing as well as natural stabilizing (capping) agents in the process of NPs synthesis process.[9] However, few previous researchers also demonstrated that silver and ZnO NPs have been synthesized using microbes such as bacteria (Streptococcus mutans and Lactobacillus), fungi (Pichia fermentans JA2), algae (Gracilaria edulis) and plants (Heritiera fomes and S. apetala) that offer numerous benefits in pharmaceutical associations.[10-13]

However, biocompatibility and toxicity of NPs strongly depend on their physiological parameters such as particle size, shape, concentration, surface charge, and subsequent NPs stability.[14] The tiny-sized NPs could accumulate to higher levels in plants and be more toxic than larger ones.[15] These small-sized NPs when enter into the root cells may disturb the balance between oxidant–antioxidant processes and induce the generation of reactive oxygen species (ROS) which causes cytotoxicity and genotoxicity.[16] The excess generation of ROS induced by NPs could damage the biomolecules and organelles structures leading to protein oxidative carbonylation, lipid peroxidation, breakage DNA/RNA strands, protein damage, and membrane destruction in cells consequently leading to necrosis, apoptosis, and even mutagenesis.[17] The oxidative stress and the ROS generation induced by silver nanoparticles (AgNPs) in tomato (*Solanum lycopersicum* L.) plants and ZnONPs in bacterium (*Deinococcus radiodurans*) has been documented.[18,19]

Among various plant organs, *Allium cepa* root tip is the first organ that comes in direct contact with the NPs and it has been used for evaluating chromosomal aberrations (CAs) since the 1920s.[20] The NPs induced structural chromosomal alterations including DNA breaks, inhibition of DNA synthesis, and alter DNA replication.[21] Currently, there are meager literatures available on the cytological effects of AgNPs and ZnONPs on plant systems. Hence, the present investigation was undertaken to study the green synthesis and characterization of AgNPs and ZnONPs using *Garcinia livingstonei* leaf extract and their potential applications for mitotic cell division, CAs, and micronucleus formation in root meristem cells of *arietinum* hasve been reported.

MATERIALS AND METHODS

Test chemicals

Silver nitrate (AgNO3), Zinc nitrate (ZnNO3), aceto-orcein, 1N HCL, sodium hydroxide, and glacial acetic acid were procured from S. D. Fine-Chem Ltd. (Mumbai, India). UV-absorption spectra were recorded on a Jasco spectrophotometer, at the wavelength range from 200 to 800 nm with 1 nm of resolution (Jasco Corporation, Chiyoda-ku, Tokyo, Japan). Fourier transform infrared (FT-IR) spectra were recorded using PerkinElmer spectrometer (PerkinElmer, Ohio, USA) version 10.03.09 (KBr pellet technique). Powder X-ray diffraction (XRD) was recorded on an X-ray diffractometer using Cu Kα (1.5406 Å) radiation (Bruker, Karlsruhe, Germany). The surface morphology and size of the NPs were analyzed by an atomic force microscopy (AFM) (NaioAFM, QuantumDesign, Toshima-ku, Tokyo, Japan) and high-resolution transmission electron microscopy (HR-TEM) was measured using JEOL 2100F FEG microscope at an operating of 200 kV after casting a drop of ZnONPs dispersion in ethanol over Cu grid (Jeol, Akishima, Tokyo, Japan).

Preparation of plant extract

Healthy leaves of *G. livingstonei* T. Anderson (Clusiaceae) were collected from Botanical Garden of Karnatak University, campus Dharwad, Karnataka, India. The plant authentication was done by a botanist of the Department of Botany, University of Mysore, Karnataka, India. The specimen voucher number GLTAIV02 was given to the selected plant and was deposited at the herbarium of the JSS Academy of Higher Education and Research. The collected leaves were surface sterilized 2–3 times with running tap water to remove adhered dust impurities followed by sterile double-distilled water and then leaves were air-dried at room temperature for 3–4 days. About 100 g of air-dried leaves was taken and incised into small pieces and added into 250 ml beaker containing 100 ml of Milli-Q water and heated for 15–20 min at 60°C. Further, the reaction mixture was allowed to cool at room temperature. The extract obtained was filtered through Whatman No. 1 filter paper to remove the particulate matter and then filtered. The finely powdered extract was stored in an airtight in a vial at 4°C in the refrigerator for further analysis.

Green synthesis of silver and zinc oxide nanoparticles

The preliminary screenings of physicochemical parameters of silver and ZnONPs were optimized by leaf extracts of *G. livingstonei.* The optimization values are (a) 1 mM of silver and $ZnNO_3$ solution, (b) pH of the reaction mixture, and (c) incubation temperature at 60°C–80°C. To obtain AgNPs, 5 ml aqueous leaf extract was added to 95 ml of freshly prepared 1 mM $AgNO_3$ solution taken in a 250 ml Erlenmeyer flask and incubated at 60°C for 10 min in a water bath. Further, the reaction mixture was allowed to cool at room temperature and then adjusted to pH 8.0, 9.0, and 10.0 using 10% sodium bicarbonate solution. Reduction of silver ions to AgNPs was clearly observed within the next 15 min marked by the color change from light yellow to dark brown indicating the formation of AgNPs.[22]

Similarly, for the synthesis of ZnONPs, 5 ml of leaf extract was added to 95 ml of $ZnNO_3$ solution in a 250 ml Erlenmeyer flask and incubated at 80°C for 10 min in a water bath. The reaction mixture was allowed to cool at room temperature and pH was adjusted to 8.0, 9.0, and 10.0. During the reaction period, the color of the solution changed from light yellow to light brown, which indicates the formation ZnONPs and reduction of zinc ions.[23] The nanomaterials obtained were purified by several re-dispersions in deionized water and then centrifuged. The final product was a powder material which was dried overnight in an oven at 60°C.

Experimental design

Healthy and uniform *Cicer arietinum* L. (2 *n* = 16) seeds were procured from the University of Agricultural Science, Dharwad. The experiment

was conducted in accordance with a protocol standardized by Debnath *et al.* The obtained seeds were surface sterilized 3–4 times with 0.1% magnesium chloride followed by double-distilled water to remove fungal and other microbiotic contaminants. The surface-sterilized seeds were placed on moistened cheesecloth in sterile Petri dishes. When the radicals reached 2–3 cm in length, they were treated with different concentrations of AgNPs and ZnONPs solutions, namely 5, 25, 50, and 100 µg/ml for 24 h at the interval of 3, 6, 12, and 24 h along with distilled water as control.

Cytological preparations

After each treatment, the roots were cut and fixed immediately into Carnoy's fluid containing 3 parts of ethyl alcohol and 1 part of the glacial acetic acid (3:1) for 24 h. After hydrolysis in 1N hydrochloric acid for 2 min at room temperature, then they were stained with aceto-orcein stain for 5 min. Further squash was prepared for cytological analysis. The prepared slides were observed under ×40 magnification power of a compound microscope. To evaluate mitotic index (MI) and chromosomal aberrations, a minimum 500 cells were examined from both treated and control groups.[24] Based on the cytological observations, the following indices can be calculated as follows: MI is the number of dividing cells to the total number of cells, multiplied by 100, and CA is the total number of aberrant cells divided by the total number of observed cells, multiplied by 100.

Statistical analysis

The experimental statistical data were expressed as mean ± standard deviation with windows (Windows installer-KB893803-×86) SPSS IBM software version 20 (IBM, Armonk, NY, USA) statistical tools, with two way ANOVA followed by the least significant difference test to calculate the mean and SD for each parameter.

RESULTS AND DISCUSSION

Ultraviolet-visible absorption spectral analysis

As manifested in Figure 1a, the UV-visible spectra of biosynthesized AgNPs showed a prominent characteristic absorption peak at 413 nm with pH 10, evidencing that the formation of AgNPs mainly depends on pH of the reaction medium.[25,26] Similarly, in the case of ZnONPs, the absorbance peak noticed at 387 nm with pH 8 [Figure 1b] is due to the effect of surface plasmon resonance.[27] Furthermore, the observed band could be due to intrinsic bandgap absorption of ZnO and electron transitions from the valence band to the conduction band.

Infrared spectroscopy analysis

Biosynthesized AgNPs and ZnONPs using *G. livingstonei* leaf extract were analyzed by FT-IR spectra within the scan range of 4000–500 cm^{-1} The spectral data showed that the as-synthesized AgNPs exhibit (broad, sharp) peaks at 3441.85, 2924.55, 2854.89, 1742.37, 1632.12, 1462.63, and 1384.03 cm^{-1} which are depicted in Table 1, which corresponds to O-H stretch, H-bonded of the alcohols and phenols. The band at 2924.55 cm^{-1} represents the C-H stretching of aliphatic and aromatic amines.[28] The band noticed at 2854.89 cm^{-1} is assigned to asymmetric stretching and vibration in methyl groups. The band at 1742.37 cm^{-1} is attributed to C = O stretching oxidation of aromatic alcohol (e.g., polyphenols).[29] The strong peaks at 1462.63, 1384.03, and 1115.31 cm^{-1} indicated the presence of C-O stretching of aliphatic amines,–C-O-C-stretching, and aromatic amines, respectively. Similarly, in the FT-IR spectrum of as-obtained ZnONPs, the bands appeared at 3441.81, 2925.48, 2853.69, 1738.47, 1632.31, 1384.30, 1119.50, and 1041.70 cm^{-1} corresponds to O-H stretch, H-bonded of the alcohols and phenols[30] whereas a band at 2925.48 cm^{-1} was attributed to C-H stretching of hydroxyl group. The bands at 2853 and 1738.47 cm^{-1} correspond to stretch vibration in methyl groups and C = O stretching oxidation of aromatic alcohol. The absorption bands at 1632.31 and 1384.30 cm^{-1} are due to the carbonyl group, glycosidic linkage of C-O-C, and secondary alcoholic groups.[31,32] The bands at 1119.50 and 1041.70 cm^{-1} represent the C-N stretching of aliphatic and aromatic amines.[33]

X-ray diffraction analysis

The crystalline nature of the purified biosynthesized AgNPs was evaluated using powder XRD analysis [Figure 2a]. The obtained data have appeared with 2θ range of 30°–90°. From the Figure, it can be clear that the four distinct peaks at 38.39°, 44.53°, 64.13°, and 77.59° correspond to (111), (200), (220), and (311) indices, respectively, face-centered cubic (FCC) lattice of AgNPs. This result was in correlation with the Joint Committee on Powder Diffraction Standards (JCPDS) card No. 04–0783. The as-obtained AgNPs showed a characteristic high-intensity peak at (111) lattice plane with the average size of the NPs was calculated to be 14.6 nm using the Debye–Scherrer equation, $D = K\lambda/\beta Cos\theta$. On the other hand, the XRD spectrum of as-synthesized ZnONPs showed

Table 1: Infrared spectroscopy absorption peaks and their associated functional groups involved in the biosynthesis of silver nanoparticles and zinc oxide nanoparticles

Absorption peaks (cm^{-1})		Functional groups
AgNPs	ZnONPs	
3441.85	3441.81	O-H stretch, H-bonded of the alcohols and phenols
2924.55	2925.48	C-H stretching of hydroxyl group
2854.89	2853.69	Stretch vibration in methyl groups
1742.37	1738.47	C=O stretching oxidation of aromatic alcohol
1632.12	1632.31	Amide I linkage due to carbonyl stretch in proteins
1462.63	1461.58	C-O stretching of aliphatic amines
1384.03	1384.30	–C-O-C- stretching
1115.31	1041.70	Aromatic amines

ZnONPs: Zinc oxide nanoparticles; AgNPs: Silver nanoparticles

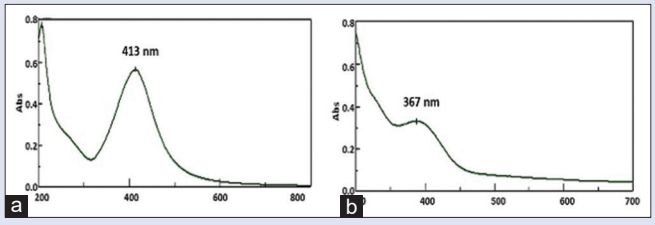

Figure 1: Ultraviolet-visible spectra of (a) Silver nanoparticles and (b) zinc oxide nanoparticles showing absorption band at 413 and 367 nm, respectively

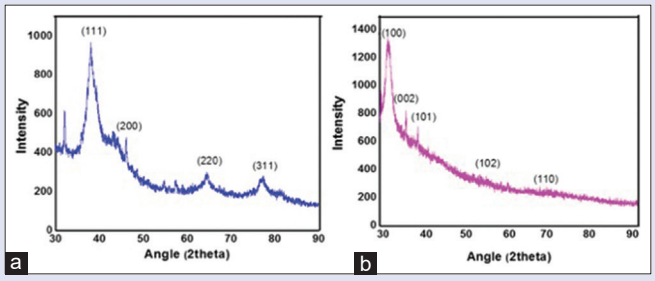

Figure 2: X-ray diffraction of as-obtained (a) Silver nanoparticles and (b) Zinc oxide nanoparticles

that four distinct peaks at 31.86°, 37.78°, 43.98°, 64.18°, and 77.14° can be indexed as (111), (111), (200), (220), and (311) planes of FCC in ZnONPs [Figure 2b]. XRD data are well coordinated with the existing JCPDS File No. 04–0783.[34]

Atomic force microscopy

The size and shape of the AgNPs and ZnONPs were estimated on the basis of AFM measurements. Figure 3a and b represent the two-dimensional and three-dimensional images of synthesized AgNPs and ZnONPs. From this Figure, it can be clearly seen the topological appearance and distribution of NPs. However, maximum surface particle size of the AgNPs is affirmed within 23.74 nm and ZnONPs have 74.12 nm with spherical and irregular in shape.

High-resolution transmission electron microscopy analysis

The HR-TEM images of as-prepared AgNPs and ZnONPs are depicted in Figure 4a and b. The size and shape of NPs were confirmed by HR-TEM images that they are spherical and irregular in shape. The size of AgNPs was found to be between 5 and 65 nm at pH 10 and ZnONPs were in the range of 38–94 nm at pH 8. The obtained nanostructures are highly crystalline in nature, showing lattice fringes, and the extent of agglomeration is very less.

Genotoxic analysis

The present study evaluates the comparative analysis of the clastogenic/genotoxic effect of as-prepared AgNPs and ZnONPs. [Figures 5 and 6 and Tables 2 and 3]. To assess the toxicity of NPs, the root tip cells of *C. arietinum* were used and treated with the different concentrations, namely 5, 25, 50, and 100 µg/ml for 24 h at the interval of 3, 6, 12, and 24 h of AgNPs and ZnONPs. Double-distilled water was used as a control. From the experimental data, it was seen that the value of MI was found to be highest (74.33 ± 1.30) in the control and for AgNPs, it was 2.00 ± 0.52 at 100 µg/ml for 24 h duration of exposure, whereas ZnONPs exhibit highest (49.33 ± 1.52) mitotic activity when compared to control. In 24 h treatment, the inhibitory rate was increased (2.00 ± 0.05) at 100 µg/ml. The tested materials were determined statistically significant at $P < 0.05$ when compared to the control [Tables 2 and 3]. It means the MI of AgNPs and ZnONPs was decreased with increasing the concentrations of NPs at different stages, namely prophase, metaphase, anaphase, and telophase of the cell cycle. Previous literatures showed that the decrease in MI is probably due to the mitodepressive effect for both AgNPs and ZnONPs.[35-37] This further intervenes in the normal process of mitosis resulting in the inhibition of DNA synthesis,[38] or blocking G2 phase of the cell cycle.[39] Debnath *et al.* (2018) reported similar results using both silver and gold NPs on *A. cepa* root tip cells. An increase in the concentration of AgNPs could damage the DNA in lung cancer cells (A549) through the generation of ROS in mitochondrial membranes reported previously.[40] Thus, treatment using NPs can decrease cell viability, inhibits ATP synthesis, and increases lactate dehydrogenase leakage in both TK6 and HepG2 cells.[41]

The genotoxic effect of as-obtained AgNPs and ZnONPs was manifested by the appearance of several types of cytological abnormalities (structural and numerical anomalies). The highest frequency of chromosomal anomalies in cells exposed to AgNPs was observed at 100 µg/ml after which there was a decline in the frequency of CAs in case of ZnONPs [Tables 2 and 3]. From the results, it is evident that the total percentage of abnormal cells was increased as the concentration of both biogenic AgNPs and ZnONPs and the duration of exposure increased when compared to control. Further, the obtained results in the present study are similar to that of observed by Kumari *et al.*[42] and Ghosh *et al.*[43] in hydroponically cultivated *A. cepa* root tip cells. This shows that the aberration induced by AgNPs and ZnONPs was caused in a concentration and time-dependent manner and induction of various kinds of mitotic abnormalities such as micronucleus, sticky chromosomes, bridges, multipolar anaphase, laggard, and c-metaphase presented in the microscopic images [Figures 5 and 6]. The most frequently occurred chromosomal anomalies are micronucleus followed by stickiness at the higher concentration of AgNPs and ZnONPs. The formation of micronuclei (MNi) is the most effective and reliable assay to determine the genotoxicity in plant systems. Thus, maximum percentages of MNi induced by biogenic AgNPs in *C. arietinum* root cells could originate from acentric chromatid/chromosome fragments that fail to be integrated to any of the daughter nuclei during mitosis or meiosis.[44] The most frequently occurring chromosomal abnormalities

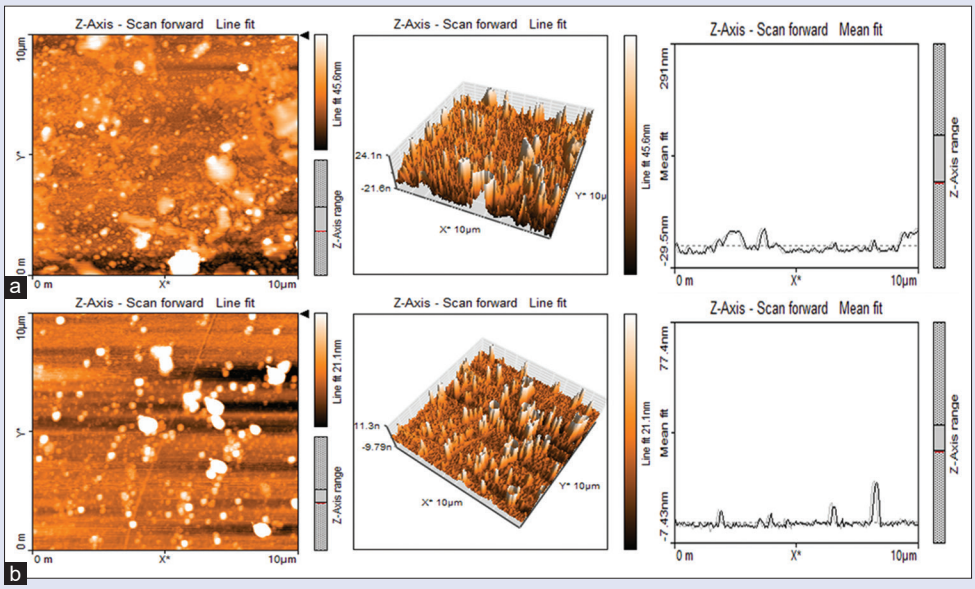

Figure 3: Atomic force microscopy analysis of (a) Silver nanoparticles and (b) Zinc oxide nanoparticles shown with a magnification of 10 µM

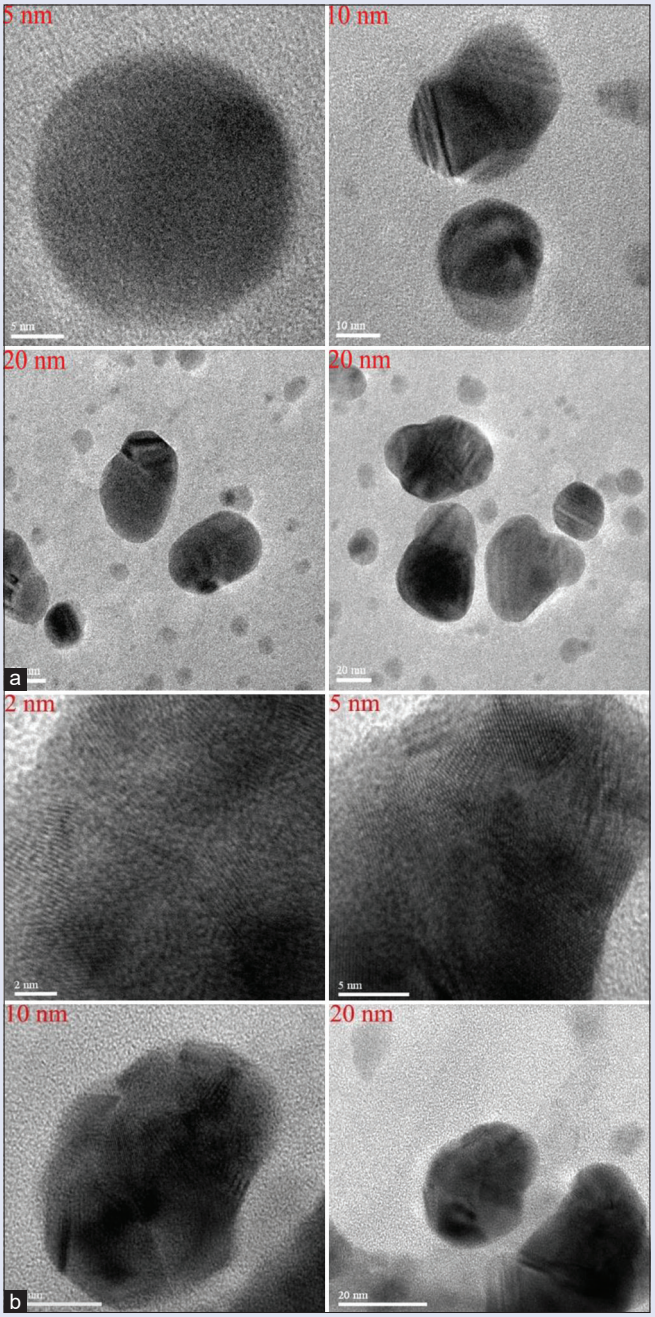

Figure 4: High-resolution transmission electron microscopy images of as-prepared (a) Silver nanoparticles and (b) zinc oxide nanoparticles shown with various magnifications, namely 2, 5, 10, and 20 nm

were recorded in the different mitotic phases treated with AgNPs and ZnONPs. Chromosome stickiness can cause serious changes in nucleic acids (DNA or RNA) resulting in the inappropriate folding of the chromosome fiber into a single chromatid which can lead to breakage of the DNA chain.[45] El-Ghamery and Mousa suggested that the sticky chromosomes can cause incomplete separation of daughter chromosomes and subsequently, the process of cell division occurs irregularly, with few chromosomes not adhering to the chromosomal assembled complex and being lost during the cell cycle.[46] The formation of chromosomal bridge at anaphase was observed in the treatment of AgNPs and ZnONPs. Further, the obtained results were statistically significant at $P < 0.05$.

Furthermore, the induction of chromosomal bridge could be due to the effect of AgNPs and ZnONPs in treated root tip cells. The occurrence of chromosomal bridges could be attributed to the breaking and rejoining of chromatin fibers which can lead to the formation of acentric (lacking a centromere) fragments and dicentric chromosomes (two centromeres) bridging at anaphase.[47] Multipolar anaphases were recorded with low frequencies in *C. arietinum* root tip cells treated with AgNPs and ZnONPs. Moreover, the AgNPs induced the highest multipolar anomalies in the concentration of 100 µg/ml at 24 h duration of exposure when compared to ZnONPs. This type of anomaly may induce due to the splitting of spindle apparatus in different directions so the chromosomes spread sporadically in the cell.[48] Laggard chromosome induction is due

Table 2: Mitotic index and chromosomal aberrations of *Cicer arietinum* root cells treated with different concentrations of silver nanoparticles

Treatment period (h)	Concentration (µg/ml)	MI (%±SD)	Number of cells examined	Abnormal anaphase						CAs %±SD
				Stickness	c-mitosis	MN	Bridge	Laggard	Multipolar	
Control ($D.H_2O$)		77.60±1.24	500	-	-	-	-	--	-	-
$AgNO_3$		75.30±1.16	500	-	-	-	-	-	-	-
3	5	74.33±1.30	500	12	-	-	1		-	4.33±0.88
		68.73±0.61	500	15	-	-	3	2	-	6.66±0.88
		64.66±1.13	500	17	2	-	2	1	-	7.33±0.04
		61.26±1.51	500	15	3	-	4	2	-	8.00±0.29
6	25	51.40±1.70	500	18	4	1	3	2	-	9.00±0.56
		45.60±2.20	500	17	4	3	2	1	-	11.66±0.57
		39.73±1.50	500	21	3	3	4	3	1	12.00±0.29
		31.60±2.10	500	19	4	3	6	3	1	9.00±0.56
12	50	23.73±0.50	500	23	5	4	8	5	1	12.00±0.29
		21.33±1.02	500	20	5	3	7	4	3	14.00±0.92
		18.73±0.61	500	22	6	5	9	5	4	14.66±0.77
		16.40±1.11	500	26	7	7	13	6	7	21.66±0.88
24	100	10.06±0.61	500	24	9	6	11	8	7	22.00±3.46
		6.00±1.40	500	27	9	8	9	8	8	24.00±0.92
		3.13±0.61	500	32	10	8	15	10	8	30.00±0.00
		2.00±0.52	500	35	13	9	11	12	10	33.00±0.46

$P<0.05$ in LSD test. MI: Mitotic index; CAs: Chromosomal aberrations; SD: Standard deviation; LSD: Least significant difference; MN: Micronucleus

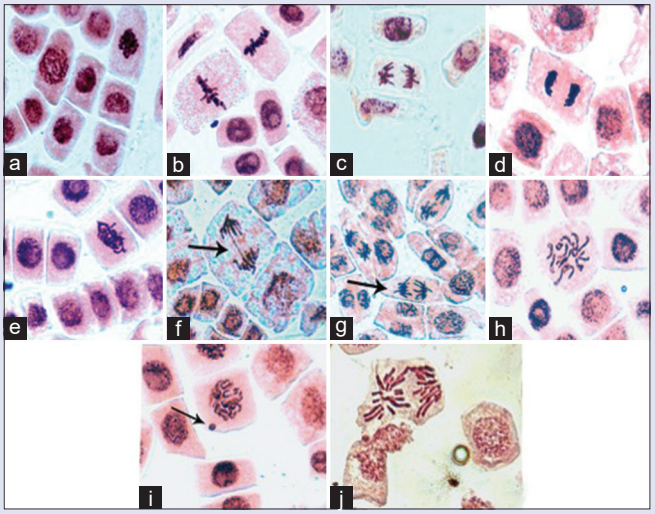

Figure 5: Mitotic chromosomes and chromosomal aberrations observed for *Cicer arietinum* root cells treated with silver nanoparticles synthesized using leaf extract of *Garcinia livingstonei* (a-d) normal mitotic stages, (e) sticky chromosome, (f) bridges, (g) laggard, (h) c-metaphase, (i) micronucleus, and (j) multipolar anaphase, scale bar-5µm

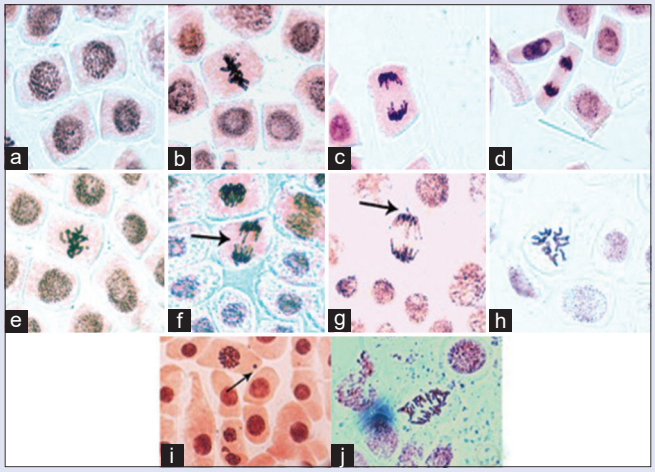

Figure 6: Mitotic chromosomes and chromosomal aberrations observed for *Cicer arietinum* root cells treated with as-obtained zinc oxide nanoparticles synthesized using leaf extract of *Garcinia livingstonei* (a-d) normal mitotic stages, (e) sticky chromosome, (f) bridges, (g) laggard, (h) c-metaphase, (i) micronucleus, and (j) multipolar, scale bar-5µm

to failure of spindle fiber alignment and one or few of the chromosomes lags behind the other chromosomes moving toward the spindle poles.[49,50] In metaphase, the induction of c-metaphase was recorded in *C. arietinum* root tip cells treated with the AgNPs and ZnONPs. Thus, AgNPs increased the percentage of c-metaphase when compared with the control at all concentrations and duration of exposure. The occurrence of c-metaphase can be resulted from the action of aneugenic effect (loss of entire chromosome)[51] of the NPs resulting to induce the risk of aneuploidy and causes an irreversible effect to the cell leads to cell death.[52] Most importantly, the present study showed that the percentage of abnormalities induced by AgNPs in *C. arietinum* was higher than that of ZnONPs, which is dose and duration dependent. Similar effects of NPs on root growth of *A. cepa,*[53] *Allium sativum,*[54,55] *Triticum sativum,*[56] *Drimia polyantha*,[57] and *Pisum sativum*[58] were reported by several authors in the previous studies. Therefore, higher treatment and duration of exposure of AgNPs and ZnONPs to *C. arietinum* causes CAs, cellular dysfunctions, and generate intracellular ROS, which ultimately induces oxidative imbalance leading to mitodepressive and genotoxic effects in the plant cells.

CONCLUSION

In summary, a reliable, eco-friendly, cost-effective, and rapid green synthesis of AgNPs and ZnONPs using *G. livingstonei* leaf extract is reported. The size of the synthesized AgNPs was found in the range of 5–65 nm and ZnONPs were between 38 and 94 nm with the spherical nature. The biological efficacy of as-obtained AgNPs and ZnONPs was tested on *C. arietinum* root meristems and was found to be significantly active. The higher concentration of AgNPs had a marked decline in MI and was found to be associated with a significant increase in abnormality index when compared to ZnONPs. Both the prepared NPs caused major changes in intracellular components into the root cell, leading to

Table 3: Mitotic index and chromosomal aberrations of *Cicer arietinum* root cells treated with different concentrations of zinc oxide nanoparticles

Treatment period (h)	Concentration (µg/ml)	MI (%±SD)	Number of cells examined	Abnormal anaphase						CAs %±SD
				Stickness	c-mitosis	MN	Bridge	Laggard	Multipolar	
Control ($D.H_2O$)		56.33±2.41	500	-	-	-	-	--	-	-
$ZnNO_3$		52.21±1.23	500	-	-	-	-	-	-	-
3	5	49.33±1.52	500	-	-	-			-	-
		45.80±0.40	500	4	-			1	-	0.66±0.01
		43.00±1.05	500	4	-	-		1	-	1.66±0.57
		40.40±0.91	500	7	-	-		3	-	2.66±0.52
6	25	32.13±0.30	500	11	-	-	3	2	-	6.66±2.08
		28.40±0.91	500	13	-	1	2	2	-	8.00±0.46
		26.06±0.61	500	15	1	3	3	4	-	10.00±0.04
		23.86±0.50	500	14	3	6	5	3	-	12.33±0.61
12	50	19.66±1.02	500	16	5	6	7	5	1	14.00±0.29
		16.60±2.02	500	19	4	5	7	4	1	21.66±2.08
		11.20±0.91	500	22	7	4	8	6	3	21.00±3.46
		9.13±0.83	500	26	7	7	10	6	5	22.66±3.05
24	100	5.26±0.61	500	25	11	8	9	7	5	23.33±2.88
		3.33±0.50	500	27	9	7	9	7	4	25.00±2.00
		3.13±0.06	500	22	8	7	10	10	7	28.06±0.25
		2.00±0.05	500	29	11	8	13	11	7	29.72±2.19

$P<0.05$ in LSD test. MI: Mitotic index; CAs: Chromosomal aberrations; SD: Standard deviation; LSD: Least significant difference; MN: Micronucleus

remarkable damage to the DNA and cell division. Moreover, both the NPs arrest the cell division at various phases of cell cycle and induce the formation of chromosomal abnormalities such as micronucleus, sticky chromosomes, bridges, multipolar anaphase, laggard, and c-metaphase. Therefore, it can be concluded that the synthesized ZnONPs were found to be more effective genetically as well as environmentally safe and nontoxic than the AgNPs.

Acknowledgements

The authors are thankful to the Chairman P. G. Department of Botany, Karnatak University, Dharwad, India, for providing necessary laboratory facilities. The authors are also grateful to the University Grants Commission, New Delhi, India, for financial assistance under by UGC- DSA-I phase program (No. F.4-29/2015/DSA-I (SAP-II) dated 09-03-2015) of the department. The authors are also thankful to USIC- KUD, for instrumentation facility. KSP thankfully acknowledges the Director, Amrita Vishwa Vidyapeetham, Mysuru campus, for infrastructure support. CS acknowledges the support and infrastructure provided by the JSS Academy of Higher Education and Research (JSSAHER), Mysuru, India. The author extends their appreciation to The Researchers Supporting Project number (RSP-2020/201) King Saud University, Riyadh, Saudi Arabia.

Financial support and sponsorship

University Grants Commission, New Delhi, India, for financial assistance under by UGC- DSA-I phase program (No. F.4-29/2015/DSA-I (SAP-II) dated 09-03-2015).

Conflicts of interest

There are no conflicts of interest.

REFERENCES

1. John MS, Nagoth JA, Ramasamy KP, Mancini A, Giuli G, Natalello A, *et al.* Synthesis of bioactive silver nanoparticles by a pseudomonas strain associated with the antarctic psychrophilic protozoon *Euplotes focardii*. Marine Drugs 2020;18:38.
2. Sahana R, Daniel K, Sankar SG, Archunan G, Vennison SJ, Sivakumar M. Formulation of bactericidal cold cream against clinical pathogens using *Cassia auriculata* flower extract-synthesized Ag nanoparticles. Green Chem Lett Rev 2014;7:64-72.
3. Hussain A, Oves M, Alajmi MF, Hussain I, Amir S, Ahmed J, *et al.* Biogenesis of ZnO nanoparticles using *Pandanus odorifer* leaf extract: Anticancer and antimicrobial activities. RSC Adv 2019;9:15357-69.
4. Meruvu H, Vangalapati M, Chippada SC, Bammidi SR. Synthesis and characterization of zinc oxide nanoparticles and its antimicrobial activity against *Bacillus subtilis* and *Escherichia coli*. J Rasay Chem 2011;4:217-22.
5. Chauhan R, Reddy A, Abraham J. Biosynthesis of silver and zinc oxide nanoparticles using *Pichia fermentans* JA2 and their antimicrobial property. Appl Nanosci 2015;5:63-71.
6. Mandava K. Biological and non-biological synthesis of metallic nanoparticles: Scope for current pharmaceutical research. J Pharm Sci 2017;79:501-12.
7. Khandel P, Yadaw RK, Soni DK, Kanwar L, Shahi SK. Biogenesis of metal nanoparticles and their pharmacological applications: Present status and application prospects. J Nanostruct Chem 2018;8:217-54.
8. Madkour LH. Biogenic-biosynthesis metallic nanoparticles (MNPs) for pharmacological, biomedical and environmental nanobiotechnological applications. Chronic Pharm Sci 2018;2:384-444.
9. Singh J, Dutta T, Kim K, Rawat M, Samddar P, Kumar P. Green' synthesis of metals and their oxide nanoparticles: Applications for environmental remediation. J Nanobiotechnol 2018;16:84.
10. Kasraei S, Sami L, Hendi S, AliKhani MY, Rezaei-Soufi L, Khamverdi Z. Antibacterial properties of composite resins incorporating silver and zinc oxide nanoparticles on *Streptococcus mutans* and *Lactobacillus*. Rest Dent Endod 2014;39:109.
11. Chauhan R, Reddy A, Abraham J. Biosynthesis of silver and zinc oxide nanoparticles using *Pichia fermentans* JA2 and their antimicrobial property. Appl Nanosci 2014;5:63-71.
12. Priyadharshini RI, Prasannaraj G, Geetha N, Venkatachalam P. Microwave-mediated extracellular synthesis of metallic silver and zinc oxide nanoparticles using macro-algae (*Gracilaria edulis*) extracts and its anticancer activity against human PC3 cell lines. Appl Biochem Biotech 2014;174:2777-90.
13. Thatoi P, Kerry RG, Gouda S, Das G, Pramanik K, Thatoi H, *et al.* Photo-mediated green synthesis of silver and zinc oxide nanoparticles using aqueous extracts of two mangrove plant species, *Heritiera fomes* and *Sonneratia apetala* and investigation of their biomedical applications. J Photochem Photobiol B Biol 2016;163:311-8.
14. Li X, Wang L, Fan Y, Feng Q, Chui F. Biocompatibility and toxicity of nanoparticles and nanotubes. J Nanomat 2012;548389:19.
15. Rastogi A, Zivcak M, Sytar O, Kalaji HM, He X, Mbarki S, *et al.* Impact of metal and metal oxide nanoparticles on plant: A critical review. Front Chem 2017;5:78.
16. Tripathi DK, Ahmad P, Sharma S, Chauhan DK, Dubey NK. Nanomaterials in plants, algae and microorganisms: Concept and controversies. Acad Press 2018;2:382.
17. Yu Z, Li Q, Wang J, Yu Y, Wang Y, Zhou Q, Li P. Reactive oxygen species-related nanoparticle toxicity in the biomedical field. Nanoscale Res Lett 2020;15:115.
18. Çekiç FÖ, Ekinci S, İnal MS, Ünal D. Silver nanoparticles induced genotoxicity and oxidative

stress in tomato plants. Turk J Boilo 2017;41:700-7.

19. Singh R, Cheng S, Singh S. Oxidative stress-mediated genotoxic effect of zinc oxide nanoparticles on *Deinococcus radiodurans*. 3 Biotech 2020;10:66.
20. Grant WF. Chromosome aberration assays in *Allium*. A report of the US environmental protection agency gene-tox program. Mutat Res 1982;99:273-91.
21. Nefic H, Musanovic J, Metovic A, Kurteshi K. Chromosomal and nuclear alterations in root tip cells of *AlliumCepa* L. induced by alprazolam. Med Arh 2013;67:388-92.
22. Prathna TC, Chandrasekaran N, Raichur AM, Mukherjee A. Biomimetic synthesis of silver nanoparticles by *Citrus limon* (lemon) aqueous extract and theoretical prediction of particle size. Colloids Surf B Biointer 2011;82:152-9.
23. Naseer M, Aslam U, Khalid B, Chen B. Green route to synthesize zinc oxide nanoparticles using leaf extracts of *Cassia fstula* and *Melia azadarach* and their antibacterial potential. Sci Rep 2020;10:9055.
24. Debnath P, Mondal A, Hajra A, Das C, Mondal NK. Cytogenetic effects of silver and gold nanoparticles on *Allium cepa* roots. J Genetic Eng Biotech 2018;16:519-26.
25. Suman TY, Rajasree SR, Kanchana A, Elizabeth SB. Biosynthesis, characterization and cytotoxic effect of plant mediated silver nanoparticles using *Morinda citrifolia* root extract. Colloids Surf B Biointer 2013;106:74-8.
26. Moldovan B, Sincari V, Perde-Schrepler M, David L. Biosynthesis of silver nanoparticles using *Ligustrum ovalifolium* fruits and their cytotoxic effects. J Nanomat 2018;8:627.
27. Nithya K, Kalyanasundharam S. Effect of chemically synthesis compared to biosynthesized ZnO nanoparticles using aqueous extract of *C. halicacabum* and their antibacterial activity. Open Nano 2019;4:S118 -25.
28. Abdel-Raouf N, Alharbi RM, Al-Enazi NM, Alkhulaifi MM, Ibraheem IB. Rapid biosynthesis of silver nanoparticles using the marine red alga *Laurencia catarinensis* and their characterization. J Basic Appl Sci 2018;7:150-7.
29. Baranwal A, Chiranjivi AK, Kumar A, Dubey VK, Chandra P. Design of commercially comparable nanotherapeutic agent against human disease-causing parasite, *Leishmania*. Sci Rep 2018;8:8814.
30. Mydeen SS, Raj Kumar R, Kottaisamy M, Vasantha VS. Biosynthesis of ZnO nanoparticles through extract from *Prosopis juliflora* plant leaf: Antibacterial activities and a new approach by rust-induced photocatalysis. J Saudi Chem Soc 2020;24:393-406.
31. Sutradhar P, Saha M. Green synthesis of zinc oxide nanoparticles using tomato (*Lycopersicon esculentum*) extract and its photovoltaic application. J Exp Nanosci 2016;11:314-27.
32. Raj A, Lawerence R. Green synthesis and characterization of ZnO nanoparticles from leafs extracts of *Rosa indica* and its antibacterial activity. Rasayan J Chem 2018;11:1339-48.
33. Tabit FT. Komolafe NT, Tshikalange TE, Nyila MA. Phytochemical constituents and antioxidant and antimstronicrobial activity of selected plants used traditionally as a source of food. J Med Food 2016;19:324-9.
34. Fakhari S, Jamzad M, Kabiri Fard H. Green synthesis of zinc oxide nanoparticles: A comparison. Green Chem Lett Rev 2019;12:19-24.
35. Kumari MS, Khan S, Pakrashi S, Mukherjee A, Chandrasekaran N. Cytogenetic and genotoxic effects of zinc oxide nanoparticles on root cells of *Allium cepa*. J Hazard Mater 2011;190:613-21.
36. Rosculete E, Olaru AL, Rosculete CA, Bonciu E. Assessment of cytological effects of food preservative potassium metabisulphite to *Allium cepa*. Am J Plant Sci 2020;11:11-23.
37. Fadoju OM, Osinowo OA, Ogunsuyi OI, Oyeyemi IT, Alabi OA, Alimba CG, *et al.* Interaction of titanium dioxide and zinc oxide nanoparticles induced cytogenotoxicity in *Allium cepa*. Nucleus 2020;63:159-66.
38. Lafarga V, Sung HM, Haneke K, Roessig L, Pauleau AL, Bruer M, *et al.* TIAR marks nuclear G2/M transition granules and restricts CDK1 activity under replication stress. EMBO Rep 2019;20:e46224.
39. Ovejero S, Bueno A, Sacristán MP. Working on genomic stability: From the S-Phase to mitosis. Genes 2020;11:225.
40. El-Hussein A, Hamblin MR. ROS generation and DNA damage with photo-inactivation mediated by silver nanoparticles in lung cancer cell line. IET Nanobiotechnol 2017;11:173-8.
41. Demir E, Qin T, Li Y, Zhang Y, Guo X, Ingle T, *et al.* Cytotoxicity and genotoxicity of cadmium oxide nanoparticles evaluated using *in vitro* assays. Mut Res Genetic Toxicol Env Mutagen 2020;850:503149.
42. Kumari M, Mukherjee A, Chandrasekaran N. Genotoxicity of silver nanoparticles in *Allium cepa*. Sci Total Environ 2009;407:5243-6.
43. Ghosh M, Jana A, Sinha S, Jothiramajayam M, Nag A, Chakraborty A, *et al.* Effects of ZnO nanoparticles in plants: Cytotoxicity, genotoxicity, deregulation of antioxidant defenses and cell-cycle arrest. Mut Res Genetic Toxicol Environ Mutagen 2016;807:25-32.
44. Chondrou V, Trochoutsou K, Panayides A, Efthimiou M, Stephanou G, Demopoulos NA. Combined study on clastogenic, aneugenic and apoptotic properties of doxorubicin in human cells *in vitro*. J Biol Res Thessaloniki 2018;25:17.
45. Nagaonkar D, Shende S, Rai M. Biosynthesis of copper nanoparticles and its effect on actively dividing cells ofmitosis in *Allium cepa*. Biotechnol Prog 2015;31:557-65.
46. El-Ghamery AA, Mousa MA. Investigation on the effect of benzyladenine on the germination, radicle growth and meristematic cells of *Nigella sativa* L. and *Allium cepa* L. Ann Agric Sci 2017;62:11-21.
47. Terradas M, Martín M, Genescà A. Impaired nuclear functions in micronuclei results in genome instability and chromothripsis. Arch Toxicol 2016;90:2657-67.
48. El-Ghamery A, El-Kholy M, Abou El-Yousser M. Evaluation of cytological effects of $Zn2^{+}$ in relation to germination and root growth of *Nigella sativa* L. and *Triticum aestivum* L. Mut Res Genetic Toxicol Environ Mutagen 2003;537:29-41.
49. Bharathi T, Gnanamurthy S, Dhanavel D, Ariraman M. Induced physical mutagenesis and its effect in cytological behavior of Ashwagandha (*Withania somnifera* (L.) Dunal). Int Lett Natural Sci 2014;12:152-61.
50. Guo X, Ni J, Zhu Y, Zhou T, Ma X, Xue J, Wang X. Folate deficiency induces mitotic aberrations and chromosomal instability by compromising the spindle assembly checkpoint in cultured human colon cells. Mutagenesis 2017;32:547-60.
51. Leme DM, Marin-Morales MA. *Allium cepa* test in environmental monitoring: A review on its applications. Mutat Res 2009;682:71-81.
52. Sabeen M, Mahmood Q, Bhatti ZA, Irshad M, Bilal M, Hayat MT, *et al. Allium cepa* assay based comparative study of selected vegetables and the chromosomal aberrations due to heavy metal accumulation. Saudi J Biol Sci 2019;27:1368-74.
53. Sun Z, Xiong T, Zhang T, Wang N, Chen D, Li S. Influences of zinc oxide nanoparticles on *Allium cepa* root cells and the primary cause of phytotoxicity. Ecotoxicology 2019;28:175-88.
54. Shaymurat T, Gu J, Xu C, Yang Z, Zhao Q, Liu Y, *et al.* Phytotoxic and genotoxic effects of ZnO nanoparticles on garlic (*Allium sativum* L.): A morphological study. Nanotoxicol 2012;6:241-8.
55. Al-Ahmadi Mona S. Cytogenetic and molecular assessment of some nanoparticles using *Allium sativum* assay. Afr J Biotech 2019;18:783-96.
56. Abdelsalam NR, Abdel-Megeed A, Ali HM, Salem MZ, Al-Hayali MF, Elshikh MS. Genotoxicity effects of silver nanoparticles on wheat (*Triticum aestivum* L.) root tip cells. Ecotoxi Environ Safety 2018;155:76-85.
57. Daphedar A, Taranath TC. Characterization and cytotoxic effect of biogenic silver nanoparticles on mitotic chromosomes of *Drimia polyantha* (Blatt. and McCann) stearn. Toxicol Rep 2018;5:910-8.
58. Labeeb M, Badr A, Haroun SA, Mattar MZ, El-Kholy AS, El-Mehasseb IM. Ecofriendly synthesis of silver nanoparticles and their effects on early growth and cell division in roots of green pea (*Pisum sativum* L.). Gesunde Pflanzen 2020;72:113-27.